Student Exploration of Star Formation Rate in Three High-Redshift Galaxy Clusters:

an NOAO/Spitzer Education and Public Outreach Project

Matthew Pellegrino[1], Vinay Patel[1], Curt Collingwood[1], Clare Mundy[1], Dr. Thomas Loughran[1,2]

1: Saint Joseph's High School, South Bend, Indiana 2: Department of Physics, University of Notre Dame, Notre Dame, Indiana

Introduction

This research was conducted under the Spitzer Space Telescope Research Program for Teachers and Students. Students at St. Joseph High School in South Bend, Indiana, have been lucky enough to take part in this program for the past two years, through the school's Science Research class. In this class, students are introduced to different possible projects—several of which involve the Spitzer Space and Hubble Telescopes.

Vinay Patel and Matt Pellegrino (at Spitzer Science Center, Pasadena)

Matt Pellegrino and Vinay Patel were the first St. Joe students to work with star formation rates. As a part of this project, Pellegrino and Patel traveled to Pasadena, California, where they had the opportunity to calculate star formation rates for three galaxy clusters at the Spitzer Science Center. Spitzer is a very useful telescope for researching SFR. Although the Hubble has better resolution, the SST can detect the hot dust which hides much star formation from visible light detection. The better resolution of the Hubble, on the other hand, provides more reliable information on cluster member morphology.

HST/ACS I-Band Image PBCD MIPS Image

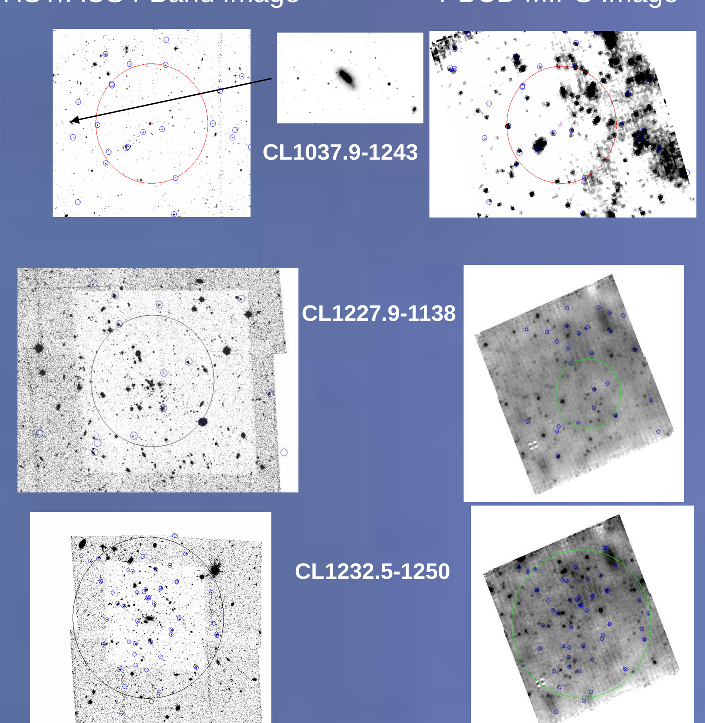

Hubble Image Spitzer Image with Flux

As part of a team including six high school teachers (John Blackwell, Velvet Dowdy, Rosa Hemphill, Ardis Herrold, Thomas Loughran, and Dwight Taylor, under the guidance of three professional astronomers (Gregory Rudnick (NOAO), Rose Finn (Siena College), and Vandana Desai (then at California Institute of Technology), Pellegrino and Patel used Hubble and Spitzer data to determine SFR for three high redshifted galaxy clusters. They assembled all of the data, their calculations, and the final star formation rates into a lengthy spreadsheet This year Clare Mundy and Curt Collingwood are advancing the project, and have inherited the task of piecing together Pellegrino's and Patel's work so as to build upon it.

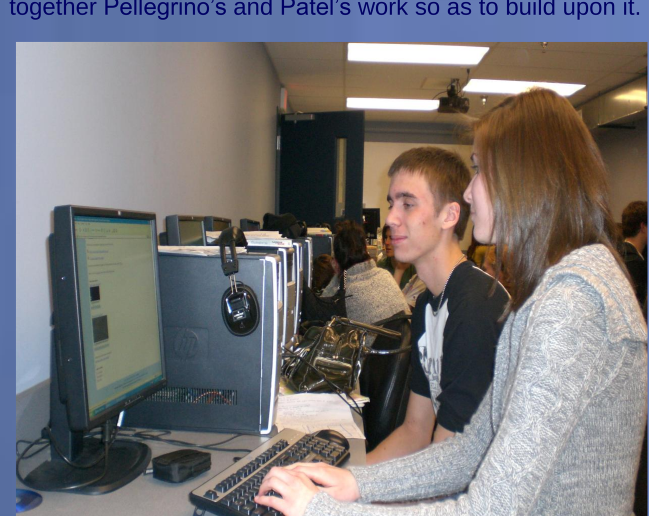

Curt Collingwood and Clare Mundy of Saint Joseph's High School Research Community

AG2 =SUM(AE2:AE46)

	A	B	C	D	E	F	G	H	I
1	EDISC ID Number	RA (Decimal)	Dec (Decimal)	Hubble Type	Flux (microJy)	Error in Flux	Photometric Ir	Spectroscopic	Luminosity
2	EDCSNJ1037521-1243392	159.4670715	-12.72756386	5	565.8	46.3	1	1	43.9733
3	EDCSNJ1038022-1242560	159.5093079	-12.71554279	7	357.8	48.5	1	-1	43.7743
4	EDCSNJ1038016-1241080	159.5064545	-12.68554497	111	884.8	131	1	-1	44.1675
5	EDCSNJ1038012-1242150	159.5049896	-12.70415878	5	334.5	47.6	1	-1	43.7451
6	EDCSNJ1037596-1243469	159.4981384	-12.7297039	-2	371.6	46.3	1	-1	43.7907
7	EDCSNJ1037590-1245212	159.4959869	-12.75588989	-7	576.8	46.5	1	-1	43.9817
8	EDCSNJ1037590-1242557	159.4959412	-12.71546745	11	210.5	46.7	1	-1	43.5439
9	EDCSNJ1037589-1245578	159.4953919	-12.76606083	4	322.1	47.4	1	-1	43.7287
10	EDCSNJ1037586-1244022	159.494278	-12.73395443	3	447.7	47.2	1	-1	43.8717

Hubble Type Key	
-7	Star
-6	Very Compact; Can't Tell Morphology
-5	Elliptical
-2	S0 or Lenticular
1	Sa
2	Sab
3	Sb
4	Sbc
5	Sc
6	Scd
7	Sd
8	Sdm
9	Sm
10	Im
11	Irregular
66	Couldn't Tell Morphology

A1 Cluster

	A	B	C	D	E	F	G	H	I	J	K	L	M	N
1	Cluster	Coordinates (Decimal)		Redshift	Mass	Number of	Number & Percent Composition Of...				SFR	Virial Radius	Half Virial Radius	Distance
2	Name	RA	DEC	z	($M_\odot$)	Members	Ellipticals	Lenticulars	Spirals	Irregular	($M_\odot$/yr)	R_{200} (Mpc)	R_{100} (Mpc)	Conversion (Mpc/")
3	CL1037	159.46333	-12.724167	0.5789	3.906977E+13	45	4 (8.89%)	2 (4.44%)	25 (55.6%)	2 (4.44%)	3872.5851	0.567655	0.283828	23.68
4	CL1227	186.97458	-11.638139	0.6355	2.261580E+14	26	1 (3.85%)	1 (3.85%)	17 (65.4%)	1 (3.85%)	1948.1839	0.996517	0.498259	24.72
5	CL1232	188.12708	-12.843333	0.5414	1.610196E+15	55	5 (9.09%)	1 (1.82%)	22 (40.0%)	3 (5.45%)	3114.4763	1.990197	0.995098	22.92

The following sections are reproduced from Pellegrino's and Patel's RBSE paper.

Star Formation Rate in Three High-Redshift Galaxy Clusters: A Contribution to the Study of Galactic Evolution

Vinay Patel and Matt Pellegrino

Saint Joseph's High School, South Bend, IN

Teacher: Dr. Thomas Loughran

Abstract

By analyzing data taken from the Spitzer Space Telescope, star formation rates (SFRs)—a key indicator that varies greatly over the lifecycles of galaxies—have been calculated for each of the 127 galaxies of three high-redshift clusters (cl1037, cl1227, cl1232, z = 0.54 to 0.64). (These three galaxy clusters are part of a much larger EDisCS catalogue, which consists of thirty such clusters.) SFR estimates are arrived at by averaging across five theoretical models for determining total infrared luminosity from 15 micron luminosity, which is in turn derived from Spitzer's 24 micron flux measurements. These calculated SFRs have been compared with other data for the cluster members, such as distance from the center of the cluster and Hubble type. Furthermore, these SFRs have also been compared to the morphological distribution of other clusters of similar redshift, and there is substantial agreement.

Methodology

The procedure to calculate the star formation rate of CL1037, CL1227, and CL1232 includes the identification of cluster members; the conversion of 24 micron flux (measured using the MIPS instrument on the Spitzer Space Telescope) of those cluster members to luminosity at a specific, rest-frame wavelength; model-guided extrapolation from luminosity at the rest-frame wavelength to total infrared luminosity (L_{TIR}); and the conversion of the total infrared luminosity to SFR.

The first step to calculating SFR after attaining the data is to identify the cluster membership: we need to know which of the galaxies in the observed field belong in the cluster so we can accurately measure the SFR of the entire cluster. This is done by calculating the redshift of each galaxy and then comparing this to the redshift of the cluster. The redshift of each galaxy was calculated in two ways: spectroscopically and photometrically. The spectroscopic redshifts were calculated using the spectra of the cluster members. The shift of each galaxy's emission lines is directly related to the redshift of the galaxy, and by calculating this shift in emission lines, we can accurately estimate the redshift of a galaxy. This is the most precise method of determining the redshift, but it did not help much, in our case. Many of the individual members' galaxies are relatively faint objects, and because of this, obtaining spectral data requires much telescope time. As a result, very few of the galaxies being examined had spectra to analyze. For the remaining galaxies, photometric redshifts were used. Using two photometric codes, the publicly available HyperZ package and Gregory Rudnick's self-created code, the redshift was approximated for each galaxy. The goal of both of these codes is to estimate the galaxy's redshift based on its observed fluxes by using a standard SED fitting procedure. These codes contain a set of galaxy SEDs, or templates, for each type of galaxy (spirals, ellipticals, starbursts, etc.), that are shifted to all redshifts from 0 to 2. Then, all of these redshifted templates are compared to the SEDs of the galaxies, and depending on which template at which certain wavelength most closely matches the galaxy SED, the most likely redshift is indicated. Photometric redshifts are not as accurate as the spectroscopic ones; however, they are much easier to obtain. After finding all of the redshifts for each galaxy, we determined cluster membership by seeing whether the redshifts of the galaxies were reasonably close to the redshift of the cluster.

Once cluster membership is determined, the flux (the number of particles that flows through a unit area per unit time) detected by Spitzer must be converted to luminosity. In addition, since luminosity is a measure of the amount of energy per unit time that an object radiates at the source, whereas flux is energy detected by us, luminosity needs to be given in rest-frame wavelength and not in the observed wavelength. Thus the luminosity at 24 micron wavelengths is converted to luminosity at the rest-frame wavelength, according to the equation

$\lambda_{rest} = \lambda_{observed}/(1 + z)$.

Using this formula, where CL1037's redshift is 0.58, the rest-frame wavelength was calculated to be 15.3 microns. This information, however, is not enough to calculate SFR. The total energy emitted at wavelengths from 8 to 1000 microns, which is the total infrared luminosity (L_{TIR}), of each galaxy is required. Using a set of five model spectral energy distributions (SEDs), we can estimate this total energy output.

These models have been computed using properties of the dust in the galaxies, such as how the dust emission depends on the energy that the dust absorbs and the composition of the dust itself (i.e. density of the dust or size of grains of dust). Since galaxies are different, there are a range of models to span the entire range of possible infrared properties in the galaxies. (When compared to local galaxies, these infrared models are found to accurately describe infrared emission.) These SEDs give us the luminosity at every wavelength from 8 microns to 1000 microns, so if the luminosity at a certain wavelength is known, the entire energy output can be determined. A c value was then calculated which would convert from luminosity at a certain wavelength (in our first case, 15.3 microns) to the L_{TIR}. The c value was calculated by integrating the SED model as a function of wavelength to find the total area under the SED curve, and then dividing this value by the luminosity at the rest-frame wavelength. By multiplying the observed luminosity at the rest-frame wavelength by the c value, the total infrared luminosity was calculated.

The last step to calculating SFR is converting L_{TIR} to SFR. Assuming most of the light emitted by the newly-formed stars is absorbed by dust, the amount of light that is re-emitted in the infrared is proportional to the total number of young stars and also the SFR. Kennicutt, by observing star formation rates of nearby galaxies in the Hubble sequence, derived a set of self-consistent SFR vs. L_{TIR} conversions. The one used in our study is presented below:

SFR (M yr-1) = 4.5 x 10-44 x L_{TIR}(ergs s-1).

This equation, with others in Kennicutt's paper, has been used many times as aids to workers in the field of astronomy. Using this equation, we were able to convert from L_{TIR} to SFR, and thus calculate SFR values for each of the three clusters being examined.

Following these calculations, we examined SFR as a function of morphology. Before doing so, however, it was necessary to verify that our three clusters had typical morphologies (see Figure 2). Seeing regular morphology distributions, except for low elliptical concentrations, we proceeded to fairly compare SFR vs. morphology in our three clusters. We also examined the SFR-distance relation for each cluster (see Figure 3).

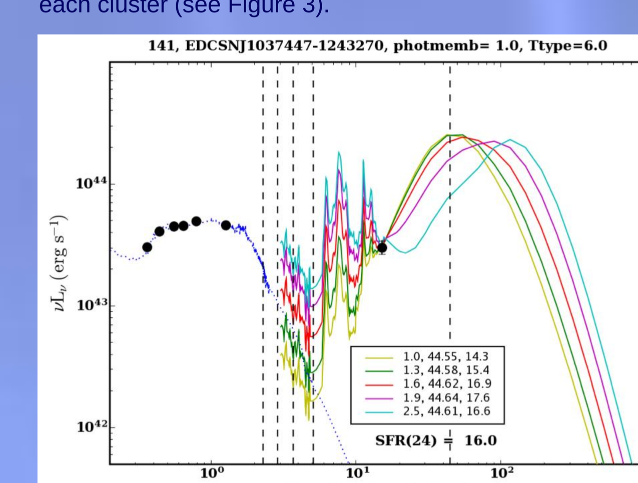

5 SED Models used to calculate SFR for CL1037

Results

In this section, we present the average SFR for objects detected by MIPS. These values, however, are not necessarily accurate, because a number of elliptical galaxies, for example, may not be detected at 24 micron wavelengths. As a result, our averages are not an average over all of the elliptical galaxies, but only an average over the elliptical galaxies that were detected by MIPS.

Using the methodology described in the previous section, we calculated the SFR for each of the cluster members in CL1037, CL1227, and CL1232. The average SFR of the five models of SFR for each of the cluster members of these clusters (in no particular order) is located at the end of the paper in Table 1, pending the application of IRAC data at V, R, I, J, and K bands to adjudicate between the five models. In addition, Figure 3 compares graphically SFR to morphology type for each cluster.

For CL1037, the average SFR per cluster member was 86.0574 M/yr. These forty five cluster members contributed to a total SFR of 3872.59 M/yr for the entire cluster. The five galaxies within half of the virial radius of the cluster totaled about 6% of the total SFR, 214.450 M/yr. We also categorized SFR according to the Hubble type for each cluster member. The elliptical galaxies detected have an average SFR of 28.4975 M/yr. The cluster's two lenticular galaxies, one of which has a particularly high SFR, averaged 312.061 M/yr, and the SFR of spiral galaxies average 81.2230 M/yr. The irregular cluster members of this cluster have an average SFR of 42.2799 M/yr.

Results, continued. . .

The average SFR per cluster member of CL1227 was 74.9301 M/yr, slightly lower than that of CL1037's. Each of these twenty six members contributed to a much lower total SFR of 1948.18 M/yr for the entire cluster. The four clusters within half of the virial radius of the cluster totaled 269.473 M/yr, about 14% of the total SFR. In this cluster, the elliptical galaxies have an average SFR of 34.1923 M/yr, lenticular galaxies have an average SFR of 30.1390 M/yr, spiral galaxies average 90.4489 M/yr, and the irregular cluster members of this cluster have an average SFR of 28.7295 M/yr.

The third cluster, CL1232, had a total SFR of 3114.48 M/yr, an average SFR of 56.6268 M/yr for each of the fifty five cluster members. From these clusters, a staggering forty seven were within half of the virial radius, totaling 2625.03 M/yr, about 84% of the total. SFR, according to the Hubble type for each cluster member, was also calculated. The elliptical galaxies detected have an average SFR of 63.5693 M/yr. Lenticular galaxies have an average SFR of 30.3968 M/yr, and the SFR of spiral galaxies average 53.3709 M/yr. The irregular cluster members of this cluster have an average SFR of 90.1752 M/yr.

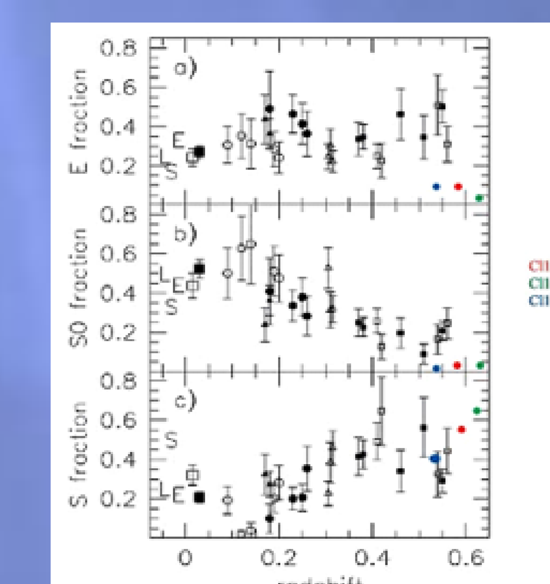

Figure From Fasano et al. (2000). The morphological classifications used in our study were given to us by Vandana Desai, who specializes in classifying galaxy morphologies. The fraction of elliptical, lenticular, and spiral galaxies is shown for clusters between z = 0 and z = 0.6, with our clusters' galaxy types shown in color. (Error analysis in progress.)

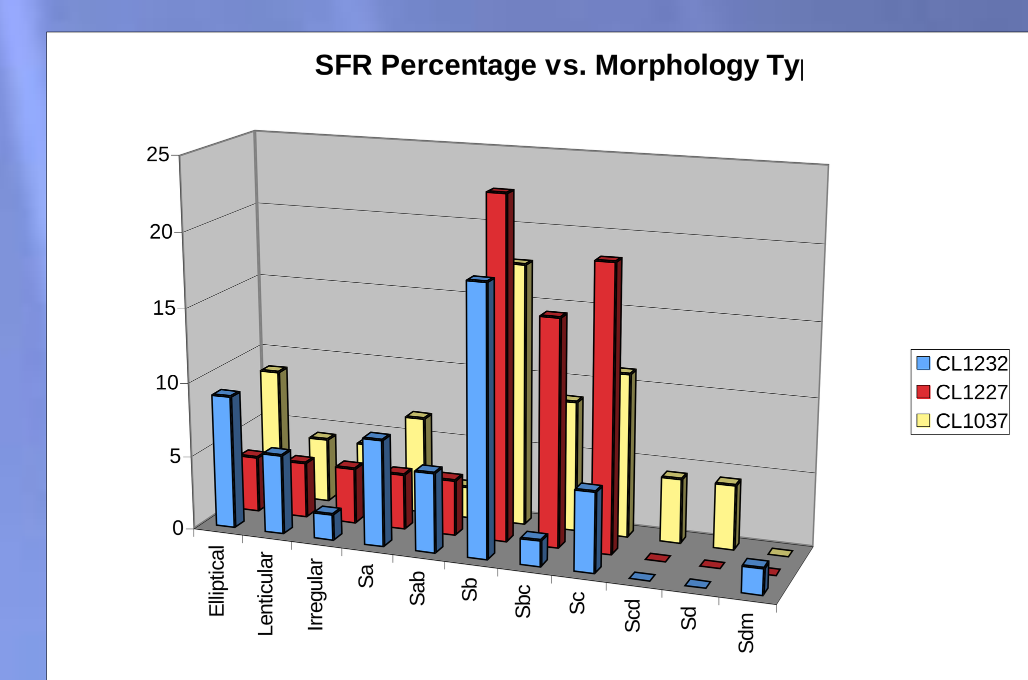

Discussion

Initially we assumed there would be generally increasing star formation rate activity within clusters of increasing redshift. Logically, this seemed sound; galaxies are younger in the past (at higher redshifts) and would seem, on average, more densely packed, giving them more star formation material—gas—closer at hand to form more stars.

We found, however, that the evolution of star formation rate within our three clusters at different redshifts did not exactly match our expectations. Instead of forming the direct relationship that was expected, we found a concave down curve for the SFR of the entire cluster, and in fact a sharp decrease in SFR as z increased for the fraction of members inside the virial radius. As a result, we need to determine whether our calculations are incorrect or whether there is a relationship more complicated than originally predicted. Our next steps will be to grapple with the reasons why our cluster's SFRs produce such interesting behavior around z = .6 or so, and whether other observational studies verify the surprising star formation variation we observed in this region.

Spitzer Space Telescope

Year 2

This year, the Science Research class has a wikispace, where all of the members of our Research Community can document all of our findings. Our Spitzer project has its own page, where we have a glossary, SFR formulas page, and also a logbook, where we record what we learn while researching our project. All of the separate project pages are linked together, so everyone in the class can easily learn about each other's projects. It has been very useful in documenting the progress we've made thus far.

As for the future of our project, there are many new angles that we can possibly take at the start of the new semester. We think it crucial that a detailed error analysis be done on the current data and SFR calculations that we have. We hope to reduce that error by eliminating some of the 5 SED models used to estimate total infrared luminosity (L_{TIR}) with Spitzer IRAC data. We also want to put together a milestone map for this project, which would make it easier for the project to be passed on to other students next year and allow them to advance the project more quickly.

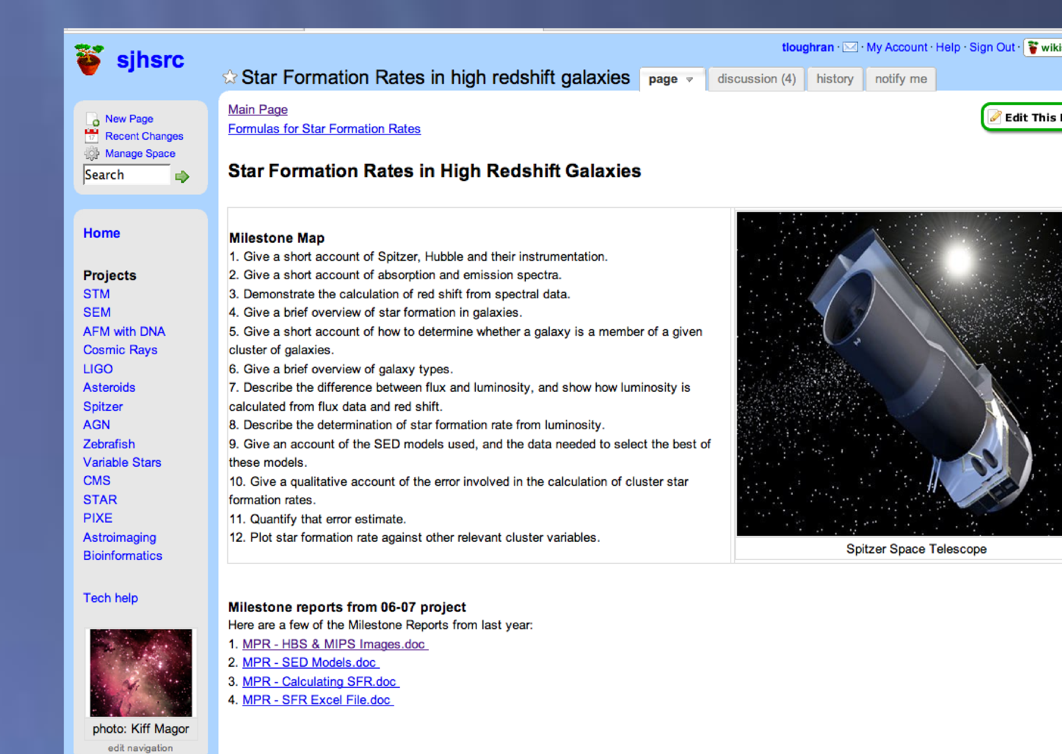

References

Finn, Rose A, et al. "Ho-Derived Star Formation Rates for Three z ≈ 0.75 EDisCS Galaxy Clusters." The Astrophysical Journal (2005): 206-277.

Finn, Rose A, et al. SFRs of 9 Intermediate-Z Clusters. Sienna College. 2006. 1-12.

Halliday, C, et al. "Spectroscopy of Clusters in the ESO Distant Cluster Survey (EDisCS)." Astronomy & Astrophysics (2004): 397-413.

Kennicutt, Robert C. "Star Formation in Galaxies along the Hubble Sequence." Annu. Rev. Astron. Astrophys. (1998): 189-231.

Poggianti, Bianca M. Color, Spectral and Morphological Transformations of Galaxies in Clusters. Padova Astronomical Observatory. The Netherlands: Kluwer Academic, 2006. 1-10.

Poggianti, Bianca M, et al. "The Evolution of the Star Formation Activity in Galaxies and Its Dependence on Environment." The Astrophysical Journal (2006): 188-215.

Poggianti, Bianca M. Emission Line Galaxies in Clusters. INAF-Padova Astronomy Observatory, Italy. 2005. 1-13.

Poggianti, Bianca M. Evolution of Galaxies in Clusters. INAF-Padova Astronomy Observatory, Italy. Novigrad: SISSA, 2004. 1-16.

Rudnick, Gregory. Agenda for Spitzer Teacher's Meeting in Pasadena CA in July 2006: 24 μm Observations of CL1037. Spitzer Teacher's Meeting, July 2006, Spitzer Science Center.

Rudnick, Gregory, et al. "Studying High Redshift Galaxy Clusters with the ESO Distant Cluster Survey." Reports From Observers: 19-24.

White, S D M, et al. "EDisCS — the ESO Distant Cluster Survey." Astronomy & Astrophysics (2005): 1-20.